



# Generation of typical meteorological years for the Argentine Littoral Region



Facundo Bre<sup>a,b</sup>, Víctor D. Fachinotti<sup>a,\*</sup>

<sup>a</sup> Centro de Investigación de Métodos Computacionales (CIMEC), Universidad Nacional del Litoral (UNL)/Consejo Nacional de Investigaciones Científicas y Técnicas (CONICET), Predio “Dr. Alberto Cassano”, Colectora Ruta Nacional 168, Paraje El Pozo, 3000 Santa Fe, Argentina

<sup>b</sup> Grupo de Investigación en Mecánica Computacional y Estructuras (GIMCE), Facultad Regional Concepción del Uruguay, Universidad Tecnológica Nacional (UTN), Ing. Pereira 676, E3264BTD Concepción del Uruguay, Entre Ríos, Argentina

## ARTICLE INFO

### Article history:

Received 16 February 2016

Received in revised form 29 July 2016

Accepted 1 August 2016

Available online 2 August 2016

### Keywords:

Typical meteorological year

Argentine Littoral Region

Southeastern South America

Zhang–Huang solar radiation model

Building energy simulation

## ABSTRACT

This work describes the generation of the typical meteorological year (TMY) for 15 locations all around the Littoral Region in northeastern Argentina, southeastern South America. The originally available weather data at each location contain, among others, dry-bulb and dew-point temperatures, wind velocity, and total sky cover, hourly measured during the period 1994–2014 by the National Meteorological Service (SMN) of Argentina. From other sources, two of these locations have hourly measured solar radiation during a few years. These radiation measurements were used to calibrate an existing Zhang–Huang solar radiation model that was then used to calculate the hourly solar radiation for the entire weather data base.

Once we complete the long-term weather database at a given location, we define the typical meteorological year (TMY) at this location as the concatenation of 12 typical meteorological months (TMM). The typicality of a month is measured using Finkelstein–Schafer statistics based on nine daily indices (maximum, minimum and mean dry-bulb and dew-point temperatures, maximum and mean wind velocity, and global solar radiation).

We finally show an example of application of the current TMYs for building energy simulation in a location deep inside Littoral. Subsequently we show the importance of the newly developed local TMY above using original TMY from neighbouring locations.

© 2016 Elsevier B.V. All rights reserved.

## 1. Introduction

This paper aims to define the typical weather for locations throughout the Argentine Littoral Region (hereinafter referred to as “Littoral”). Littoral is a region with an area of 0.5 million km<sup>2</sup> in northeastern Argentina, southeastern South America, see Fig. 1. Its climate is Cfa (C for warm temperate, f for fully humid, a for hot summer) according to the Köppen–Geiger classification [1]. In a finer classification [2], Littoral is divided into three bioclimatic zones (those ones separated by red dashed lines in Fig. 1): very hot in the north (I), hot in the center (II), and warm temperate in the south (III). Further, each zone is divided into two subzones (a and b), those ones separated by a green dashed line in Fig. 1, regarding the daily temperature range be larger or smaller than 14 °C.

Temperatures throughout Littoral are not only high to very high during summer, but also they will be 2–4.5 °C higher (throughout

southeastern South America) by 2100 according to the 2014 report of the Intergovernmental Panel on Climate Change (IPCC) [3]. Up to our knowledge, there is no information to quantify the concomitant increase in energy consumption for cooling in Littoral nor in South America, but studies in the USA indicates that the electricity used for residential cooling will increase by roughly 5–20% (depending on the location and customer class) per 1 °C warming [4].

In Littoral, the National Meteorological Service (SMN) of Argentina measures dry-bulb and dew-point temperatures, wind velocity, total sky cover, etc. on an hourly basis. For this work, they provided us these weather data for fifteen stations throughout Littoral (see Fig. 1) during the period 1994–2014.

SMN databases lack solar radiation, for which there are not long-term, continuous, frequent enough records in Argentina. Actually, the systematic record of solar radiation in Argentina began in 2010 [5] with the work of the GERSolar research group. GERSolar operates a series of solarimetric stations, one of them being located at Paraná (Littoral). For the current work, the available information on solar radiation include the data from GERSolar at Paraná (bioclimatic zone IIb, Fig. 1) during 2010–2014 and the data recorded at

\* Corresponding author.

E-mail address: [vfachinotti@intec.unl.edu.ar](mailto:vfachinotti@intec.unl.edu.ar) (V.D. Fachinotti).

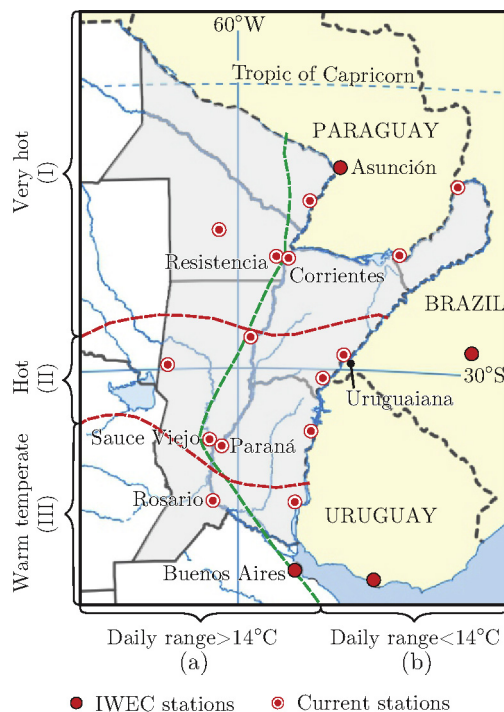


**Fig. 1.** Map of the Argentine Littoral Region (in light grey), showing the bioclimatic zones (I, II or III, a or b) and the location of weather stations. (For interpretation of reference to color in this figure legend, the reader is referred to the web version of this article.)

Corrientes (bioclimatic zone Ib, Fig. 1) by GER (research group on renewable energies) during 2010–2012.

One of the main goals of the current work is to overcome the lack of experimental solar radiation data by the use of accurate models. Following the ASHRAE development of IWEC [6] and IWEC2 [7], we evaluate two regression-based models: the Kasten model [8] and the Zhang–Huang model [9]. By fitting the available measurements as well as data from the IWEC files of neighbour locations (Asunción-Paraguay and Buenos Aires-Argentina) and satellite-derived data from the Surface meteorological and Solar Energy (SSE) database [10], we will demonstrate that the Zhang–Huang model with coefficients calibrated to Paraná is very well suited to estimate the long-term solar radiation throughout Littoral.

With the aid of such solar model, we complete the available long-term databases for 15 locations in Littoral, opening the way to the definition of the typical weather at each location, which is the final goal of this work. For accurate energy calculations at a given location, we need to know the typical local weather at short intervals (usually, every hour) all along a year judged to be typical over a long period of time. There are two general approaches to define such typical year: (1) to select a continuous, 12-month period as typical; or (2) to select each typical calendar month separately, and then to concatenate the 12 typical months to build the typical year.

The first approach was introduced in the 1970s, with examples as the Test Reference Year (TRY) from the National Climatic Center (NCC) in USA [11], and the Example Weather Year (EWY) from the Chartered Institution of Building Services (CIBS) in UK [12]. This approach excludes the extreme conditions found in the long-term weather records, producing excessively moderate typical years.

To avoid this, we decided to use the second approach, following the pioneering work of Hall et al. [13] in Sandia National Laboratories (USA). In this work, appeared in 1978, Hall et al. introduced the concept of “typical meteorological year” (TMY) as a concatenation of typical meteorological months (TMMs). Later examples are the

TMY2 [14] and TMY3 [15] from the US National Renewable Energy Laboratory (NREL), the new Test Reference Year (TRY) from the Chartered Institution of Building Services Engineers (CIBSE, former CIBS, UK) [16], the International Weather for Energy Calculations (IWEC [6,17] and IWEC2 [7]) from the American Society of Heating, Refrigerating and Air-Conditioning Engineers (ASHRAE), etc. For reviews comparing these methods, we refer to the works of Crawley and Huang [18], Lhendup and Lhundup [19], and Chan [20].

Typical years from all around the world (1042 locations in the USA, 71 locations in Canada, and more than 1000 locations in 100 other countries) are given in the EnergyPlus weather data website [21]. There you can find files defining the typical year at each location, derived from 20 sources including Sandia’s TMY [13], NREL’s TMY2 [14] and TMY3 [15], and ASHRAE’s IWEC [6,17]).

In this large database, there are very few locations in southeastern South America: Argentina, Paraguay, Uruguay, and Rio Grande do Sul (the Brazilian region neighboring Littoral) are represented by only one location each one. The shortage of information on the typical weather is a great obstacle for the development of energy simulation. Focusing on building energy simulation (BES), most of the works in Argentina [22–24] concerns short periods of time, using actual (not typical) weather data. In 2013, when we had to apply BES for Sauce Viejo (in Littoral, within the climatic zone IIb, see Fig. 1) [25], the local typical year was approximated by that one at Uruguaiana (southern Brazil). The typical years for Uruguaiana and other 410 Brazilian locations were defined by Roriz [26]. At this time, this seemed to be the best choice considering the similarity in weather conditions. However, Roriz [26] warned about the low representativeness of the typical years he defined due to the short length of historical records.

Then, we decided to generate the typical year for Sauce Viejo [27] based on the weather data measured by SMN at this location during the period 2000–2013, supplemented by solar radiation computed using the Zhang–Huang model [9] calibrated to tropical climate [28], as recommended by Kim et al. [29] for eastern Texas (USA), where the climate is Cfa like in Littoral.

Now, with the larger (in time and space) weather databases (including radiation) built at the beginning of this work, typical years are generated for the 15 locations throughout Littoral.

To this end, we follow the original method of Hall et al. [13] (the so-called “Sandia method”) for the Typical Meteorological Year (TMY). A TMY is a set of 12 typical meteorological months (TMMs). As first proposed by Hall et al. [13] and later picked up by Thevenard and Brunge [6] for IWEC generation, the typicality of a month is measured using Finkelstein–Schafer statistics based on nine daily indices (maximum, minimum and mean dry-bulb and dew-point temperatures, maximum and mean wind velocity, and global solar radiation). Each variable is given a weight considering how determinant it is for the selection of the TMM. The Sandia and the IWEC generation methods use different sets of weights, to be compared in this work.

After generating the TMYs, we give an insight of the typical weather for locations in different bioclimatic zones of Littoral (warm temperate, hot, and very hot). Finally, we develop an application to building energy simulation (BES) to highlight the importance of using the local TMY for a location deep inside Littoral.

## 2. Description of the weather data source

The meteorological database supporting this work was obtained by SMN during the period 1994–2014 at 15 weather stations located all around Littoral, those ones listed in Table 1 and shown in Fig. 1.

The available data include, among others, hourly measures of the following meteorological variables:

**Table 1**  
Geographical coordinates and altitude of the weather stations of the Argentine National Meteorological Service (SMM) throughout the Argentine Littoral Region.

Location	Latitude [S]	Longitude [W]	Altitude [m.a.s.l.]
Ceres	29°52′	61°57′	88
Concordia	31°18′	58°10′	38
Corrientes	27°26′	58°45′	62
Formosa	26°12′	58°13′	60
Guauguaychú	33°00′	58°37′	21
Iguazú	25°43′	54°28′	270
Monte Caseros	30°16′	57°39′	54
Paraná	31°46′	60°28′	78
Paso de los Libres	29°40′	57°09′	70
Posadas	27°22′	55°58′	125
Pcia. R. Sáenz Peña	26°49′	60°27′	92
Reconquista	29°10′	59°42′	53
Resistencia	27°27′	59°03′	52
Rosario	32°55′	60°46′	25
Sauce Viejo	31°42′	60°49′	18

1. Dry-bulb temperature (DBT)
2. Dew-point temperature (DPT)
3. Wind velocity (WV)
4. Relative humidity (RH)
5. Total sky (or cloud) cover (TSC)
6. Wet-bulb temperature
7. Wind direction
8. Atmospheric pressure
9. Ceiling height

These raw databases may contain missing observations, i.e., unmeasured variables for certain hours. Since the available measured data will serve as input for solar radiation models in Section 2.1, we use the data-filling methods adopted by NREL for the generation of the National Solar Radiation Database (NSRDB) [30]: gaps up to 5 h are filled by linear interpolation, while gaps from 6 to 47 h are filled with data for identical hours from adjacent days.

After this filling stage, databases may still contain missing observations for longer gaps. At this point, a decision has to be made about the usefulness of such databases. In this work, we will keep the database containing all the weather measurements for a given month of a year at a given location only if it meets the screening criteria suggested by ASHRAE [31] for the calculation of the climatic design conditions, that is:

1. the hours with measured + filled DBT are at least 85% of the total hours of this month, and
2. the difference between day and night hours with measured + filled DBT is less than 60.

Regarding the data available for this work, the total cloud cover (TSC) is the variable having the most hours without measurements. Since TSC is a crucial variable for the computation of solar radiation (that in turn is crucial for defining the typical year), it is judicious to extend the criterion 1) to TSC.

The database for a given month of a year at a given location that satisfies all these criteria is called “usable” (and it will be supplemented with modelled solar radiation as described in the following section), otherwise it is discarded.

Notice that a usable database may still contains unfilled gaps. In this case, the gap can be filled using data extracted from the same period from other years as suggested by Skeiker [32]. Fortunately, such gaps were not found in the current usable databases.

The number of usable databases for each location in Littoral and for each calendar month in the period 1994–2014 is shown in Table 2. Note that there are at least 14 usable databases for each

month and each location, which is highly satisfactory realising that ASHRAE [31] requires at least 8 years of data for each calendar month at a given location for climatic design calculations.

## 2.1. Solar radiation

This section aims to supply the just defined usable database with solar radiation. The experimental data at our disposal consist of hourly measurements of solar radiation at two locations in Littoral (Paraná and Corrientes) during a few years (2010–2014 and 2010–2012, respectively). Consequently, the measured solar radiation is not enough to complete the weather databases throughout Littoral during 1994–2014. But it is large enough to calibrate regression-based solar radiation models, specifically the Kasten model [8] and the Zhang–Huang model [33].

In Sections 2.1.1 and 2.1.2, we introduce these models, then calibrate their coefficients to make them fit the available radiation measurements, and finally evaluate the goodness of such fit. Next, in Section validation, we show that the Zhang–Huang model with coefficients calibrated for Paraná is the best suited to fit the available experimental data, and, finally, validate its extension to long periods and to the whole region.

### 2.1.1. Kasten model

This model, developed by Kasten and Czeplak [8], defines the global solar radiation on the horizontal surface, say GHSR, as the following power function of the total sky cover TSC:

$$\text{GHSR} = \text{GHSR}^0 \left[ 1 - c_1 \left( \frac{\text{TSC}}{8} \right)^2 \right] \quad (1)$$

where GHSR is given in  $\text{W}/\text{m}^2$ , TSC is given in oktas, and  $\text{GHSR}^0$  is GHSR under cloudless sky, which is fitted at its turn by the equation

$$\text{GHSR}^0 = c_3 \sin SA - c_4, \quad (2)$$

where SA is the solar altitude angle, depending on the local latitude, the hour of the day, and the date [31].

Kasten and Czeplak [8] determined the scalar coefficients  $c_i$  in Eqs. (1) and (2) to fit the measured solar radiation at Hamburg (Germany) during 1964–1973.

In this work, we compute two sets of  $c_i$  depending on the location and year which experimental data is the target of fitting: Paraná during 2013 or Corrientes during 2010. The chosen year for each location is that one having the most comprehensive radiation database. By this way, we define two Kasten models: One, say K–P, has coefficients calibrated for Paraná during 2013, and the other, say K–C, has coefficients calibrated for Corrientes during 2010.

For either case, we compute first the coefficients  $c_3$  and  $c_4$  by solving a linear least-square problem using a reflective Newton algorithm [34], and secondly the coefficients  $c_1$  and  $c_2$  by solving a non-linear regression problem using the Levenberg–Marquardt algorithm [35]. The so-computed coefficients are listed in Table 3, together with the correlation factor (R) and the Root Mean Square Error (RMSE) measuring the goodness of the fit.

Both models are good to fit the corresponding experimental data, as seen in Fig. 2. This conclusion is supported by the values of R and RMSE displayed in this figure (compared, for instance, to those ones obtained by Zhang [33] based on 24 Chinese locations:  $R=0.97$  and  $\text{RMSE}=80 \text{ W}/\text{m}^2$  for the best case).

### 2.1.2. Zhang–Huang model

Zhang and Huang [9] defined the global solar radiation on the horizontal surface at the hour  $h$  as:

**Table 2**

Number of years with usable weather databases in the period 1994–2014 for each calendar month for 15 weather stations in the Argentine Littoral Region.

Location	Month											
	J	F	M	A	M	J	J	A	S	O	N	D
Ceres	15	16	16	17	17	16	17	16	17	15	15	14
Concordia	17	17	19	20	20	19	19	19	19	16	17	16
Corrientes	19	19	19	20	21	21	21	21	20	20	18	19
Formosa	16	15	16	18	18	17	18	20	18	16	14	14
Galeguaychú	20	20	20	21	20	20	20	20	19	20	19	20
Iguazú	19	18	18	20	19	18	19	19	19	19	19	19
Monte Caseros	17	16	17	18	18	18	17	16	18	16	17	17
Paraná	18	18	18	20	20	19	19	20	18	17	17	18
Paso de los Libres	16	16	16	17	16	16	15	16	16	17	15	17
Pcia. R. Sáenz Peña	15	15	15	16	15	15	15	16	14	15	15	15
Posadas	20	20	19	21	20	20	20	20	20	20	20	20
Reconquista	16	16	17	19	18	18	19	18	18	17	16	17
Resistencia	20	20	20	21	20	20	20	20	20	20	20	20
Rosario	19	20	20	21	18	20	19	20	16	18	17	18
Sauce Viejo	19	18	18	20	20	20	20	19	19	18	18	19

**Table 3**

Coefficients, correlation factor (*R*), and root mean square error (RMSE) for the Kasten model fitted to measured hourly radiation at Paraná during 2013 and at Corrientes during 2010.

Model (location/year)	<i>c</i> <sub>1</sub>	<i>c</i> <sub>2</sub>	<i>c</i> <sub>3</sub>	<i>c</i> <sub>4</sub>	<i>R</i>	RMSE
K-P (Paraná/2013)	0.6983	3.0716	1041.1	47.146	0.975	65.28
K-C (Corrientes/2010)	0.7623	3.5316	1060.4	62.065	0.956	89.25

$$\text{GHSR} = \max \left( 0, z_1 + I_0 \sin SA \times \left[ z_2 + z_3 \frac{\text{TSC}}{8} + z_4 \left( \frac{\text{TSC}}{8} \right)^2 + z_5(\text{DBT} - \text{DBT}_{h-3}) + z_6 \text{RH} + z_7 \text{WV} \right] \right), \tag{3}$$

where GHSR is given in W/m<sup>2</sup>, the total sky cover TSC is given in oktas, the dry-bulb temperature DBT is given in degrees Celsius (°C), the relative humidity RH is given in percentage, the wind speed WV is given in m/s, SA is the solar altitude angle, *I*<sub>0</sub> = 1355 W/m<sup>2</sup> is the solar constant, and *z*<sub>1</sub>, *z*<sub>2</sub>, . . . , *z*<sub>7</sub> are adjustable scalar coefficients; note that all the weather variables in the above equation are measured at hour *h*, except DBT<sub>*h*-3</sub> that is the dry-bulb temperature measured 3 h earlier. In a later work, Zhang [33] obviates the influence of wind speed on solar radiation, a simplification that is adopted in this work.

As done for the Kasten models in Section 2.1.1, we compute the coefficients *z*<sub>*i*</sub> separately to fit the hourly measured solar radiation at Paraná during 2013 and Corrientes during 2010, giving rise to the ZH-P and ZH-C models, respectively.

For each model, we solve a linear least-square problem using a reflective Newton algorithm [34] to compute the coefficients *z*<sub>1</sub>, *z*<sub>2</sub>, . . . , *z*<sub>6</sub> (*z*<sub>7</sub> = 0 following Zhang [33]) listed in Table 4.

Again, each model is good to fit the corresponding hourly measured solar radiation, as shown in Fig. 3.

2.1.3. Solar radiation model for Littoral

Up to this point, we have shown that both the Kasten model and the Zhang–Huang model fit well the available solar radiation measurements. To avoid duplicity, we keep only the Zhang–Huang model for the remainder of this work. Note that the adoption of the Zhang–Huang model rather than the Kasten model is coincident with the criterion used by ASHRAE for the generation of IWEC2 [7], and by Kim et al. [29] for modelling the hottest and most humid portion of Texas (USA).

Now, we aim to validate the application of the currently-calibrated Zhang–Huang models to long periods and to the whole Littoral region.

**Extension to long periods.** In order to ensure the long-term validity of the ZH-P and ZH-C models, we take as reference the monthly average global horizontal solar radiation at Corrientes

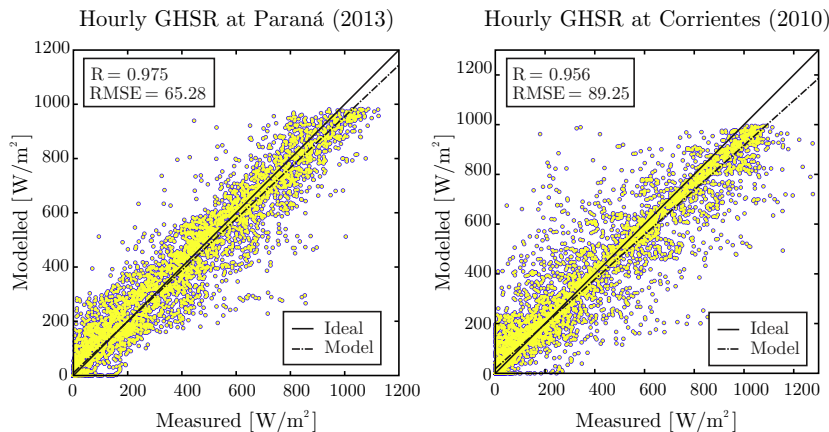


**Fig. 2.** Kasten model: fit of the measured hourly global horizontal solar radiation (GHSR) at Paraná during 2013 and Corrientes during 2010.



**Table 4**  
Coefficients, correlation factor ( $R$ ), and root mean square error (RMSE) for the Zhang–Huang radiation model fitted to measured hourly global horizontal solar radiation at Paraná during 2013 and at Corrientes during 2010.

Model (location/year)	$z_1$	$z_2$	$z_3$	$z_4$	$z_5$	$z_6$	$R$	RMSE
ZH-P (Paraná/2013)	4.0042	0.8651	0.1627	−0.4871	0.0047	−0.0038	0.979	60.10
ZH-C (Corrientes/2010)	5.1676	0.9004	0.4674	−0.7650	0.0161	−0.0050	0.961	83.93

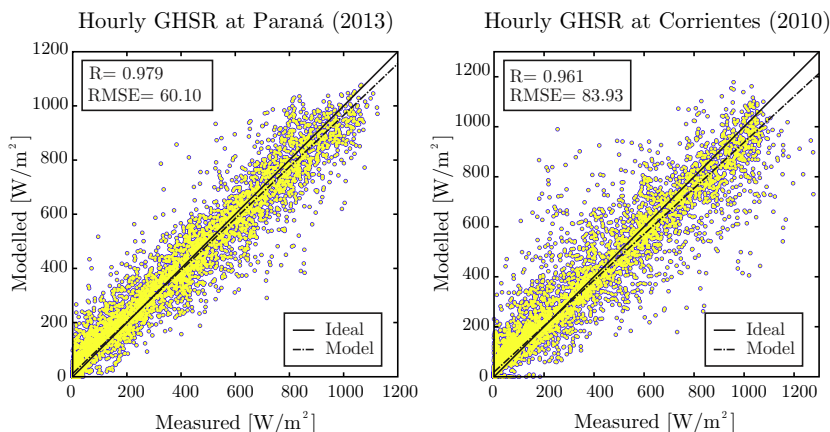


**Fig. 3.** Zhang–Huang radiation model: fit of the measured hourly global horizontal solar radiation (GHSR) at Paraná during 2013 and Corrientes during 2010.

and Paraná derived from satellite measurements along 22 years (1983–2005), given in the Surface meteorological and Solar Energy (SSE) database [10].

For Corrientes, the long-term monthly average radiation computed using ZH-P was unexpectedly closer to the reference SSE values than the ones computed using ZH-C (see Table 5). Actually, ZH-C monthly averages were usually close to SSE monthly maxima during 1983–2005, even exceeding the SSE maximum for August. This could indicate that the measured solar radiation at Corrientes during the year 2010 (the one chosen to calibrate the ZH-C model) is atypically high. Unfortunately, we have not enough hourly measurements of solar radiation at Corrientes for other years to look for a better agreement between ZH-C and SSE.

For Paraná, ZH-P monthly averages agree very well with reference data (Table 6).

**Table 5**  
Monthly average global horizontal solar radiation at Corrientes (all the values are given in kWh/m<sup>2</sup>/day). Comparison between the results using the Zhang–Huang models calibrated to Corrientes during 2010 and to Paraná during 2013 (ZH-C and ZH-P, respectively) and those ones found in the Surface meteorology and Solar Energy (SSE) database.

Monthly average solar radiation	Month												Annual average
	J	F	M	A	M	J	J	A	S	O	N	D	
Long-term ZH-C	7.19	6.40	5.57	4.30	3.64	2.92	3.57	4.62	5.59	5.98	6.71	7.02	5.29
Long-term ZH-P	6.60	5.91	5.19	4.06	3.39	2.75	3.33	4.27	5.12	5.61	6.30	6.50	4.92
Long-term SSE	6.64	5.92	5.00	3.89	3.46	2.74	3.16	3.90	4.81	5.55	6.35	6.70	4.83
Minimum SSE	5.98	4.68	4.45	3.31	3.04	1.67	2.81	3.16	3.85	4.66	5.33	5.90	–
Maximum SSE	7.77	6.87	5.90	4.71	3.81	3.29	3.76	4.49	5.63	6.60	7.30	7.24	–

**Table 6**  
Monthly average global horizontal solar radiation at Paraná (all the values are given in kWh/m<sup>2</sup>/day). Comparison between the results using the Zhang–Huang model calibrated to Paraná during 2013 (ZH-P) and those ones found in the Surface meteorology and Solar Energy (SSE) database.

Monthly average solar radiation	Month												Annual average
	J	F	M	A	M	J	J	A	S	O	N	D	
Long-term ZH-P	6.84	5.78	5.01	3.90	2.95	2.44	2.88	3.83	4.86	5.65	6.59	6.94	4.81
Long-term SSE	6.72	6.00	5.00	3.82	3.12	2.54	2.93	3.83	4.92	5.68	6.63	6.92	4.83
Minimum SSE	5.85	4.86	3.85	3.13	2.78	2.16	2.55	2.99	3.74	4.54	5.64	5.54	–
Maximum SSE	7.80	6.84	6.00	4.58	3.49	3.05	3.52	4.37	5.46	6.36	7.49	7.54	–

In conclusion, the ZH-P model is adopted to estimate the long-term radiation at Paraná and Corrientes.

**Extension to the whole region.** To validate the extension of the ZH-P model to the whole Littoral region, we take as reference the IWECC files for two neighbouring locations: Asunción (Paraguay) and Buenos Aires (Argentina), located north and south of Littoral, respectively (see Figure 1).

These IWECC files are available for free at the EnergyPlus weather data repository [21]. They contain hourly values of dry-bulb temperature, total sky cover, relative humidity, solar radiation, etc. The solar radiation is computed as a function of the measured total sky cover using the Kasten model, as explained by Thevenard and Brunger [6,17].

The hourly global horizontal solar radiation computed using the ZH-P model (fed with dry-bulb temperature, total sky cover, and

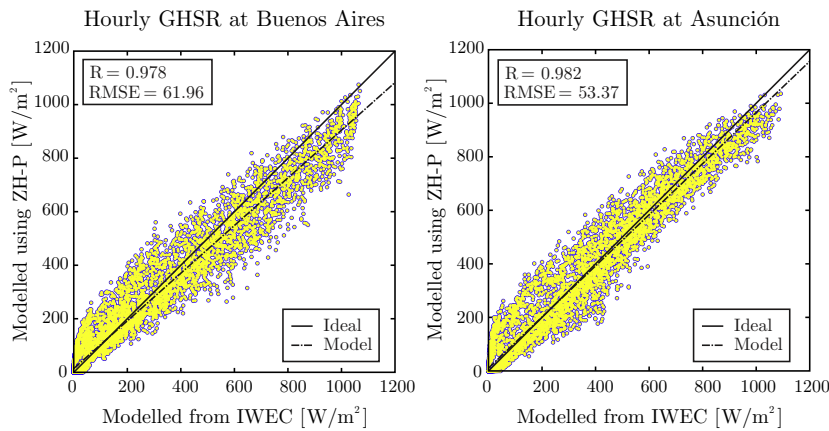


Fig. 4. Hourly global horizontal radiation at Buenos Aires (Argentina) and Asunción (Paraguay): fit of the data in the respective IWEC files using the Zhang-Huang radiation model calibrated to Paraná during 2013 (ZH-P model).

relative humidity taken from the IWEC file) agrees very well with the one found in the IWEC file, both for Asunción and Buenos Aires (Fig. 4).

As conclusion, the ZH-P model – that is, the Zhang–Huang model with coefficients calibrated to fit the measured solar radiation at Paraná during 2013 – is accurate enough (and will be used henceforth) to describe the long-term solar radiation throughout Littoral.

With the help of this model, all the usable weather databases have been supplemented with hourly global horizontal solar radiation.

### 3. Definition of the typical meteorological year

As described in the previous section, we have now a large enough number of databases containing hourly weather variables (including solar radiation) for all the calendar months in the period 1994–2014 at 15 locations throughout Littoral. In this section, we describe the process of defining the typical year for each location based on this information.

Following the method proposed by Hall et al. [13] from Sandia laboratories (from now on, referred to as the “Sandia method”), we define the typical meteorological year (TMY) as the concatenation of 12 typical meteorological months (TMMs).

#### 3.1. Definition of the typical meteorological month

Let us illustrate the process of definition of the TMM by defining the typical January for Paraná. As seen in Table 2, Paraná has eighteen usable Januarys in the period 1994–2014.

Following Hall et al. [13], we determine the closeness of each one of these Januarys, say January XXXX, to the long-term composite of all usable Januarys (or, simply, composite January) considering the nine daily meteorological indices listed in Table 7.

We characterise the behaviour of each index  $I$  along the period  $P$  using the cumulative distribution function  $CDF_I^P(x)$ , which gives the probability that  $I \leq x$  along this period. Considering the index DBTMAX for instance, its CDF along the period  $P$  is defined as:

$$CDF_{DBTMAX}^P(x) = \begin{cases} 0 & \text{if } x < DBTMAX_1, \\ (i - 0.5)/n & \text{if } DBTMAX_{i-1} \leq x \leq DBTMAX_i, \\ 1 & \text{if } x > DBTMAX_n, \end{cases} \quad (4)$$

where the  $n$  values  $DBTMAX_i$  of DBTMAX along the period  $P$  are sorted in ascending order. This is done for January

XXXX ( $P = \text{JanXXXX}$ ,  $n = 31$ ) as well as for the composite January ( $P = \text{CompoJan}$ ,  $n = 18 \times 31 = 558$  in the case of Paraná).

The CDF of DBTMAX along January XXXX is compared to the CDF of DBTMAX along the composite January using the Finkelstein–Schaffer statistics [36]:

$$FS_{DBTMAX}^{\text{JanXXXX}} = \frac{1}{31} \sum_{d=1}^{31} \left| CDF_{DBTMAX}^{\text{CompoJan}}(DBTMAX_d) - CDF_{DBTMAX}^{\text{JanXXXX}}(DBTMAX_d) \right|.$$

In a similar way, we compute FS along January XXXX for all the other indices in Table 7 (DBTMIN, DBTMEAN, DPTMAX, etc.). Then, to involve all the meteorological indices in the comparison between January XXXX and the composite January, we introduce the weighted sum of FS statistics for January XXXX:

$$WFS^{\text{JanXXXX}} = \sum_{I=1}^9 w_I FS_I^{\text{JanXXXX}}, \quad (5)$$

where  $I = 1, 2, \dots, 9$  stands for the index DBTMAX, DBTMIN, ..., GHSR, and  $w_I$  is the weight assigned to this index. Table 7 gives the values of these weights for the Sandia method [13] as well as for the IWEC generation method [6].

Once WFS is computed for all Januarys, that January with lowest WFS is the closest to the composite January in terms of CDF. According to Hall et al. [13], this January is a candidate to but not necessarily the TMM for January. The final selection of the TMM for January by Hall et al. [13] consists of three steps: (1) the five Januarys with lowest WFS are chosen as candidates; (2) those candidate Januarys with the longest run, with the most runs, and with zero runs of cloudy or warm or cool days are excluded (this is the so-called persistence criterion); and (3) the remainder candidate with the lowest WFS is the TMM for January.

But the persistence criterion may lead to excluding good candidates and even all the candidates. For this reason, Thevenard and Brunger [6] decided to ignore this criterion for the development of IWEC, and so did Huang et al. [7] for the development of IWEC2.

Since the IWECs are the most important reference for typical weather definition in South America, we follow the IWEC criterion, namely: The TMM is the month with the lowest WFS.

### 4. Results and discussion

In this section, we give the quantitative assessment of the procedure of TMM generation for all the calendar months and all the

**Table 7**  
Daily meteorological indices for the definition of the typical meteorological month and their respective weighting factors, as used by the Sandia method [13] and by the method of generation of International Weather for Energy Calculations (IWEC) [6].

Index <i>I</i>	Daily variable	Acronym	Weighting factors	
			Sandia [13]	IWEC [6]
1	Maximum dry-bulb temperature	DBTMAX	1/24	2/40
2	Minimum dry-bulb temperature	DBTMIN	1/24	2/40
3	Mean dry-bulb temperature	DBTMEAN	2/24	12/40
4	Maximum dew-point temperature	DPTMAX	1/24	1/40
5	Minimum dew-point temperature	DPTMIN	1/24	1/40
6	Mean dew-point temperature	DPTMEAN	2/24	2/40
7	Maximum wind velocity	WVMAX	2/24	2/40
8	Mean wind velocity	WVMEAN	2/24	2/40
9	Global solar radiation	GHSR	12/24	16/40

locations, which has been widely described for January at Paraná in the previous section. In Section 4.1, we compute the weighted sum of Finkelstein–Schaffer statistics (WFS) for each month of the long-term database at Paraná, as defined for a given January by Eq. (5). For each calendar month, the one having the lowest WFS is the corresponding TMM. Replicating this methodology, we determine all the TMMs for the other locations in Littoral in Section 4.2.

Then, in Section 4.3, we offer a deeper insight of the typical weather throughout Littoral by focusing on three locations within different bioclimatic regions. For these locations, the typical and the average values of the dry-bulb temperature and the global horizontal solar radiation are compared.

Finally, we apply the just generated TMY for building energy simulation at Paraná. In order to emphasize the importance of using the local weather files, we compare the results of such simulation to the results of simulating the same building using the IWEC files from Asunción and Buenos Aires. Let us remark that, before this work, these locations were the closest ones to Littoral having free and sufficiently validated typical weather files.

#### 4.1. Typical meteorological months at Paraná

First, we compute the WFS for January at Paraná using either the Sandia or the IWEC weighting factors given in Table 4; results are shown in Tables 8 and 9, respectively. Then, we complete these tables by applying the same procedure to all the other months.

**Table 8**  
Weighted sums of Finkelstein–Schaffer statistics (WFS) for all the calendar months of the year at Paraná using Sandia weighting factors; candidate months are underlined, typical meteorological months are in bold, and discarded months are indicated by ×.

Year	Month											
	J	F	M	A	M	J	J	A	S	O	N	D
1994	0.0718	0.0795	0.0947	<u>0.0696</u>	×	×	×	×	×	×	×	×
1995	×	×	×	0.0867	<u>0.0597</u>	0.1036	0.1182	0.1762	×	×	×	×
1996	×	×	×	×	0.1511	×	×	0.2002	0.1722	0.2093	×	×
1997	×	×	0.1509	<u>0.0735</u>	0.0873	0.1364	0.0926	0.0954	<u>0.0487</u>	×	0.1563	0.1310
1998	0.1690	0.1206	0.1191	0.1414	0.0898	0.0793	0.1963	0.1034	×	×	×	<u>0.0766</u>
1999	0.0951	0.0851	0.0940	0.0812	0.0526	0.1025	0.1039	0.0780	0.0553	<u>0.0583</u>	0.0970	0.0988
2000	<u>0.0542</u>	<u>0.0522</u>	×	0.1101	0.1053	0.1201	0.1196	<b>0.0449</b>	<u>0.0515</u>	0.0803	0.1040	<b>0.0467</b>
2001	0.1282	0.0997	0.1375	<u>0.0614</u>	0.1002	0.0817	<u>0.0590</u>	0.0994	0.1128	0.1485	0.0739	<u>0.0772</u>
2002	<u>0.0608</u>	0.0866	0.1425	0.1165	0.0957	0.1002	0.0930	<u>0.0511</u>	<b>0.0438</b>	0.1357	0.1000	0.1394
2003	<u>0.0672</u>	<u>0.0594</u>	<u>0.0799</u>	0.0953	<u>0.0564</u>	0.1065	0.0749	0.0861	<u>0.0517</u>	<b>0.0429</b>	<b>0.0362</b>	0.0838
2004	0.0617	0.1561	0.1275	0.1107	0.1084	<u>0.0730</u>	<b>0.0475</b>	0.0631	<u>0.0476</u>	0.0823	0.0759	0.0851
2005	<u>0.0579</u>	0.1227	0.0833	0.1050	0.0766	0.1806	0.0770	0.1024	0.1028	0.0893	0.0640	0.0803
2006	0.0641	0.0857	0.0838	<u>0.0595</u>	0.0981	<u>0.0714</u>	0.0902	<u>0.0662</u>	0.1406	0.0730	<u>0.0604</u>	0.1053
2007	0.1325	<u>0.0585</u>	0.1568	0.1187	0.1135	0.1009	0.1365	0.1136	0.1022	0.1155	0.0887	<u>0.0742</u>
2008	<b>0.0521</b>	<u>0.0738</u>	<b>0.0529</b>	0.1434	0.1152	0.1201	0.1070	0.1143	0.1062	<u>0.0529</u>	0.0862	0.0930
2009	0.1276	0.0628	<u>0.0789</u>	0.1224	0.0787	0.1453	0.1384	<u>0.0631</u>	0.0895	0.1145	0.1305	0.1532
2010	0.0975	0.1219	<u>0.0759</u>	0.0947	0.0807	<b>0.0392</b>	<u>0.0667</u>	0.0924	0.0753	0.1152	0.1006	0.1038
2011	<u>0.0585</u>	<u>0.0539</u>	0.1087	0.0815	0.0560	<u>0.0722</u>	0.0612	0.0703	0.0793	0.1121	<u>0.0469</u>	0.1131
2012	0.1415	<b>0.0455</b>	0.0554	0.0784	0.0905	<u>0.0599</u>	0.1564	0.1045	0.0653	0.1151	0.0703	0.0804
2013	0.0694	0.0916	0.0977	0.0981	<b>0.0397</b>	0.0875	<u>0.0561</u>	0.1131	0.0950	<u>0.0544</u>	0.0751	0.1079
2014	0.0855	0.1431	0.0942	<b>0.0483</b>	0.1032	0.0820	0.0957	0.0783	0.0879	<u>0.0685</u>	<u>0.0454</u>	<u>0.0766</u>

For each calendar month, the candidates for TMM according to Hall et al. [13] are the five months with lowest WFS, which are underlined in Tables 8 and 9. In this case, we found that 82% of the candidate months selected using Sandia weighting factors are coincident with those ones selected using IWEC factors.

Concerning the actual TMM for each calendar month, that one with the lowest WFS, it appears in bold in Tables 8 and 9. In this case, the TMMs chosen using either Sandia or IWEC weighting factors are the same for 10 of the 12 months.

Since we found similar results for all the locations in Littoral, this fact tends to confirm that the typical month has little sensitivity to the choice of weighting factors, either Sandia's or IWEC's, as concluded by Su et al. [37].

Consequently, we will use the IWEC weighting factors to avoid duplicity for the remainder of this work. This choice amounts to reduce the weight of solar radiation (0.4 instead of 0.5) and increase the weight of the dry-bulb temperature (0.4 instead of 0.167 for combined minimum, maximum and mean values) in the selection of the candidates, which appears to be judicious when the measured data pool for solar radiation is not as large as the one for dry-bulb temperature, as suggested by Chan et al. [38].

#### 4.2. Typical meteorological months throughout Littoral

In the previous section, we have determined the TMMs for Paraná: Those ones having the lowest WFS, which are given in bold in Table 9. Then, we apply the just-described procedure of

**Table 9**

Weighted sums of Finkelstein–Schaffer statistics (WFS) for all the calendar months of the year at Paraná using IWEC weighting factors; candidate months are underlined, typical meteorological months are in bold, and discarded months are indicated by ×.

Year	Month											
	J	F	M	A	M	J	J	A	S	O	N	D
1994	0.0703	0.0790	<u>0.0848</u>	<u>0.0632</u>	×	×	×	×	×	×	×	×
1995	×	×	×	0.0817	<u>0.0595</u>	0.0993	0.0915	0.1401	×	×	×	×
1996	×	×	×	×	0.1145	×	×	0.1653	<u>0.1423</u>	0.1536	×	×
1997	×	×	0.1333	0.0723	0.1023	0.1071	0.0956	0.0883	<u>0.0452</u>	×	0.1386	0.1198
1998	0.1952	0.1465	0.1362	0.1459	0.0906	<u>0.0748</u>	0.1767	0.1056	×	×	×	0.0904
1999	0.1336	0.0856	0.0985	0.1115	<u>0.0596</u>	0.1056	0.1091	<u>0.0687</u>	0.0712	<u>0.0591</u>	0.0798	0.0848
2000	<u>0.0611</u>	<b>0.0480</b>	×	0.0966	0.1052	0.0996	0.1378	<b>0.0444</b>	<u>0.0543</u>	<u>0.0785</u>	0.1366	<b>0.0406</b>
2001	0.1030	0.1146	0.1251	<u>0.0583</u>	0.1054	0.0851	<u>0.0512</u>	0.1132	0.1051	0.1338	0.0806	<u>0.0680</u>
2002	0.0621	0.0949	0.1294	0.1242	0.0984	0.1084	0.0948	<u>0.0470</u>	<b>0.0415</b>	0.1200	0.0836	0.1451
2003	<u>0.0553</u>	<u>0.0551</u>	<u>0.0718</u>	0.1078	<u>0.0565</u>	0.1154	<u>0.0692</u>	0.1002	<u>0.0541</u>	<b>0.0452</b>	<b>0.0357</b>	0.1147
2004	<b>0.0503</b>	0.1454	0.1311	0.0964	0.1343	<u>0.0687</u>	<b>0.0440</b>	0.0581	<u>0.0495</u>	0.0819	0.0835	0.0908
2005	<u>0.0508</u>	0.1011	0.0872	0.1194	0.0666	<u>0.1663</u>	0.0730	0.0877	0.1161	0.1085	<u>0.0540</u>	0.0791
2006	0.0783	0.0787	0.1001	<u>0.0632</u>	0.1067	0.0752	0.1092	0.0707	0.1153	0.0831	<u>0.0595</u>	0.0956
2007	0.1310	<u>0.0569</u>	0.1564	0.0967	0.1465	0.1056	0.1531	0.1442	0.0880	0.1020	0.0935	<u>0.0633</u>
2008	<u>0.0557</u>	0.0658	<b>0.0539</b>	0.1303	0.0991	0.1305	0.1232	0.1001	0.0878	<u>0.0509</u>	0.1080	0.0932
2009	0.1037	<u>0.0547</u>	0.0878	0.1336	0.0818	0.1464	0.1382	<u>0.0617</u>	0.1210	0.1155	0.1194	0.1546
2010	0.0888	0.1069	<u>0.0830</u>	0.1042	0.0778	<b>0.0433</b>	0.0731	0.1058	0.0722	0.1337	0.0898	0.1004
2011	0.0626	0.0648	0.0948	<u>0.0708</u>	<u>0.0615</u>	<u>0.0759</u>	<u>0.0678</u>	0.0862	0.0744	0.1309	0.0548	0.0902
2012	0.1257	<u>0.0498</u>	<u>0.0630</u>	<u>0.0836</u>	0.1054	<u>0.0581</u>	<u>0.1615</u>	0.0913	0.0623	0.0988	<u>0.0739</u>	<u>0.0697</u>
2013	0.0638	0.0805	0.1148	0.1010	<b>0.0432</b>	<u>0.0776</u>	<u>0.0555</u>	0.1134	0.1025	<u>0.0559</u>	0.0753	0.1435
2014	0.0822	0.1389	0.1327	<b>0.0484</b>	0.0947	<u>0.0728</u>	0.0933	0.0733	0.0936	0.0836	<u>0.0457</u>	<u>0.0705</u>

TMM generation for Paraná to all the other locations. As result, we obtain all the TMMs for all the current locations in Littoral, listed in Table 10.

Finally, at each location, the typical meteorological year is the concatenation of the 12 corresponding TMMs. In general, the TMMs for contiguous months come from different years. The consequent jumps of the weather variables at the interface of such months are eliminated by cubic spline smoothing based on the six last hours of the first month and the six first hours of the second month, as recommended by Hall et al. [13].

4.3. Typical weather in Littoral

In this section, we aim to give an insight of the typical weather through Littoral from the whole set of results of the present work. For the seek of conciseness, we choose three locations from different bioclimatic zones of Littoral to represent the whole Littoral (see Fig. 1): Resistencia (in the boundary between zones Ia and Ib, very hot with daily range of around 14 °C), Paraná (in zone IIb, i.e. hot with daily range lower than 14 °C), and Rosario (in zone IIIa, i.e. warm temperature with daily range greater than 14 °C).

To characterise the weather at these locations, we use the monthly means of the global horizontal solar radiation (GHSR) and the dry-bulb temperature (DBT) as well as the hourly means of these weather variables along January (mid-summer) and July (mid-winter).

In each case, the TMY is compared to

1. the average year, where the value of each variable at hour  $h = 1, 2, \dots, 24$  of day  $d = 1, 2, \dots, 365$  is the average of the values of this variable at hour  $h$  and day  $d$  all along the period 1994–2014 (including only the usable databases),
2. the worst year, composed by the months with highest WFS. The worst year for Paraná can be inferred from Table 9.

Results for Resistencia, Paraná, and Rosario are shown in Figs. 5, 6, and 7, respectively. For the three locations, the typical GHSR (that is, the one from the TMY) is close to the GHSR from the average year in terms of monthly means and hourly means during January and July. Furthermore, the typical hourly mean GHSR for July (mid-winter) is practically identical to the one from the average year for all the locations.

**Table 10**

Typical meteorological months (TMMs) at 15 locations in the Argentine Littoral Region.

Location	Month											
	J	F	M	A	M	J	J	A	S	O	N	D
Ceres	2005	2009	2011	2014	2011	2004	2004	2004	2008	2003	2006	2007
Concordia	2004	2011	1994	2011	2003	1998	2013	2002	2004	1997	1998	2007
Corrientes	2003	2005	2006	2012	2003	2012	2003	2005	2002	2008	2013	2007
Formosa	2005	2003	2011	2011	2011	2004	2013	2005	2002	2003	2008	2010
Guaquaychú	2003	1997	2003	1994	2003	1998	2001	2002	1995	1999	2003	2000
Iguazú	2005	2007	2010	2000	2011	2012	2003	2009	2006	2013	2000	2007
Monte Caseros	2002	2013	1994	2014	2003	2012	2013	2002	2002	2003	2005	2004
Paraná	2004	2000	2008	2014	2013	2010	2004	2000	2002	2003	2003	2000
Paso de los Libres	2000	2000	2005	2014	2003	2012	2004	1999	2002	1998	2003	2001
Pcia. R. Sáenz Peña	2005	2003	2007	2014	2013	2004	2013	2005	2004	2003	2003	2010
Posadas	2005	2013	2006	2014	2011	2012	2014	2000	2000	2001	2013	2007
Reconquista	2003	2007	2006	2006	2003	2012	2003	2002	2002	1998	1998	2010
Resistencia	2003	2005	2006	2012	2003	2012	2013	1997	2002	2013	2008	2007
Rosario	2006	2013	2008	2014	2013	2010	2013	1999	2008	1998	1996	2012
Sauce Viejo	2004	2007	2012	2006	2013	2004	2004	2004	2003	1998	2003	2012



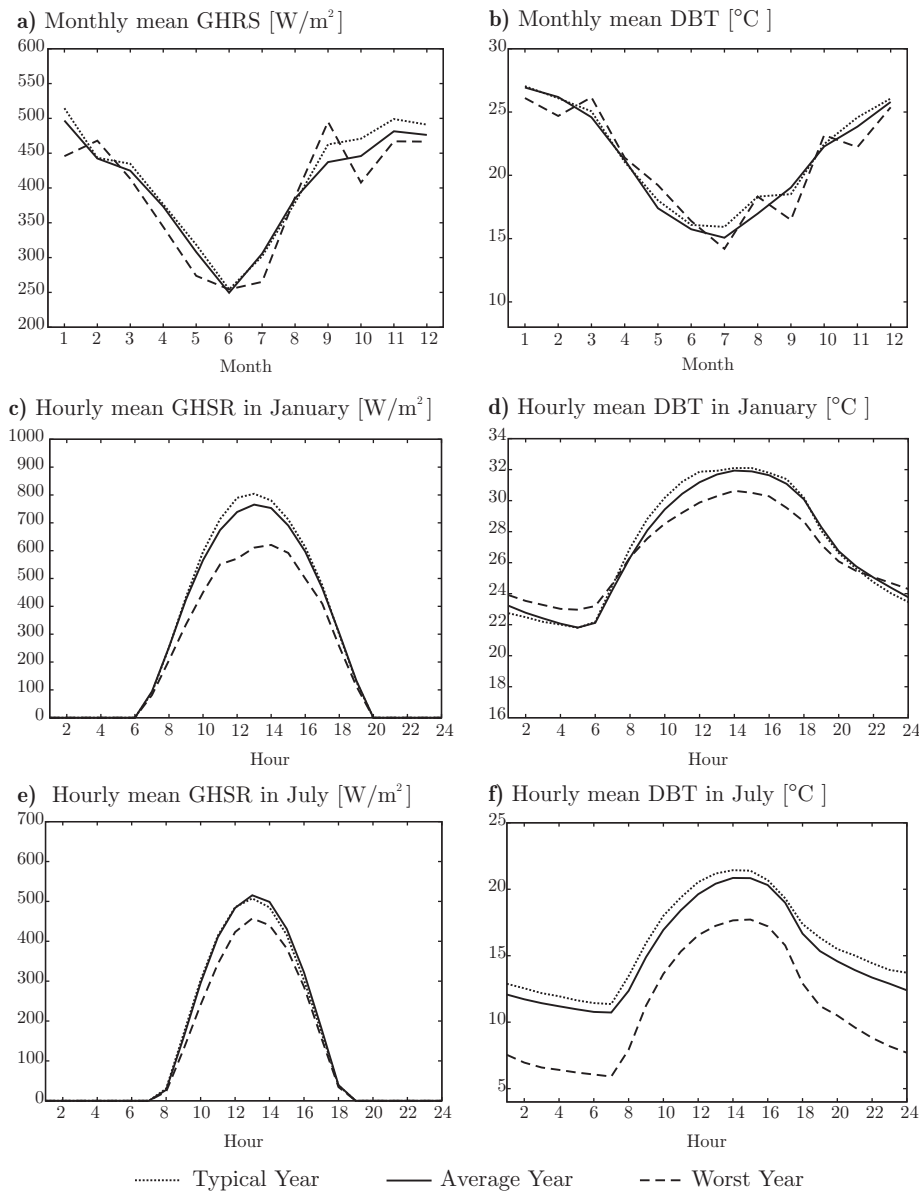


**Fig. 5.** Comparison among the typical meteorological year, the average year, and the worst year at Residencia: (a, b) monthly mean global horizontal solar radiation and dry-bulb temperature, respectively; (c, d) hourly mean global horizontal solar radiation and dry-bulb temperature, respectively, in January (mid-summer); and (e, f) hourly mean global horizontal solar radiation and dry-bulb temperature, respectively, in July (mid-winter).

Concerning dry-bulb temperature, the typical one is usually higher than the one of the average year. Differences are mostly around  $0.5\text{ }^{\circ}\text{C}$  with a peak of  $1.3\text{ }^{\circ}\text{C}$  at noon in January (mid-summer) at Rosario.

The closeness between the results for the TMY and those ones for the average year is an indicator of the validity of the current TMYs.

#### 4.4. Application to building energy simulation

Let us apply the currently defined TMYs for building energy simulation (BES) using the program EnergyPlus [39] version 8.4.0 [40].

The currently developed TMYs contain not only the weather variables entering in the TMY definition (dry-bulb and dew-point temperatures, global horizontal solar radiation, etc.) but also atmospheric pressure, wind direction, visibility, sky cover, ceiling height, precipitation, among others, from the SMN databases. For BES, we

supplemented the TMYs with illuminance using the model of Perez et al. [41], and extraterrestrial radiation following ASHRAE [31].

Then, the so-completed TMYs are converted to the EnergyPlus weather input format (EPW) by using the EnergyPlus auxiliary program Weather Converter [42]. The diffuse and direct normal radiation, key variables for BES, are added by Weather Converter by using the Perez direct/diffuse split model [41,43]. Weather Converter also gives us the Design Day according to ASHRAE [31].

To highlight the importance of using the local TMY for BES (and, by the way, to highlight the importance of the current contribution), let us apply EnergyPlus to run the BESTEST-Case 910 from ANSI/ASHRAE Standard 140-2011 [44] at Paraná. This test concerns a heavy-weight building (like most of the buildings in Littoral) with room temperature control set to  $20\text{ }^{\circ}\text{C}$  for heating and  $27\text{ }^{\circ}\text{C}$  for cooling, windows that face north (instead of south, as it would be the case for Northern Hemisphere), and 1m-horizontal overhang all along the north-facing wall at the roof level.

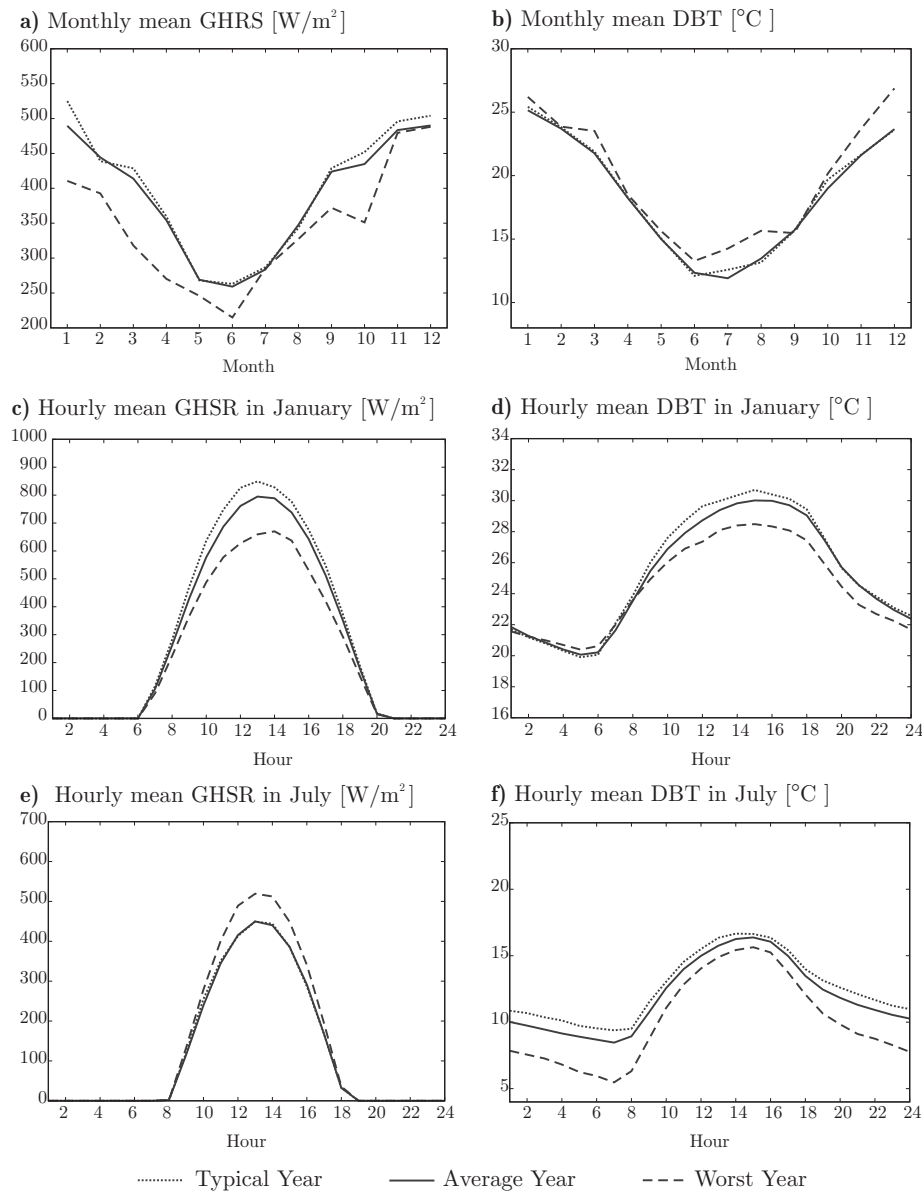


**Fig. 6.** Comparison among the typical meteorological year, the average year, and the worst year at Paraná: (a, b) monthly mean global horizontal solar radiation and dry-bulb temperature, respectively; (c, d) hourly mean global horizontal solar radiation and dry-bulb temperature, respectively, in January (mid-summer); and (e, f) hourly mean global horizontal solar radiation and dry-bulb temperature, respectively, in July (mid-winter).

Before having the typical weather file for Paraná, we would approximate it by using data from nearby locations. In our first work on BES [25], we defined the typical weather in Santa Fe (25 km northeast of Paraná) using the typical weather file of Uruguiana (southern Brazil) [26], which is located in the same bioclimatic region that Paraná and Santa Fe (see Figure 1). Unfortunately, the goodness of the typical weather file for Uruguiana is uncertain since it was defined on the base of a short pool of weather data [26]. So, we would have to approximate the typical weather at Paraná using the IWEC files of Asunción or Buenos Aires, as we are going to do now for the purpose of comparison.

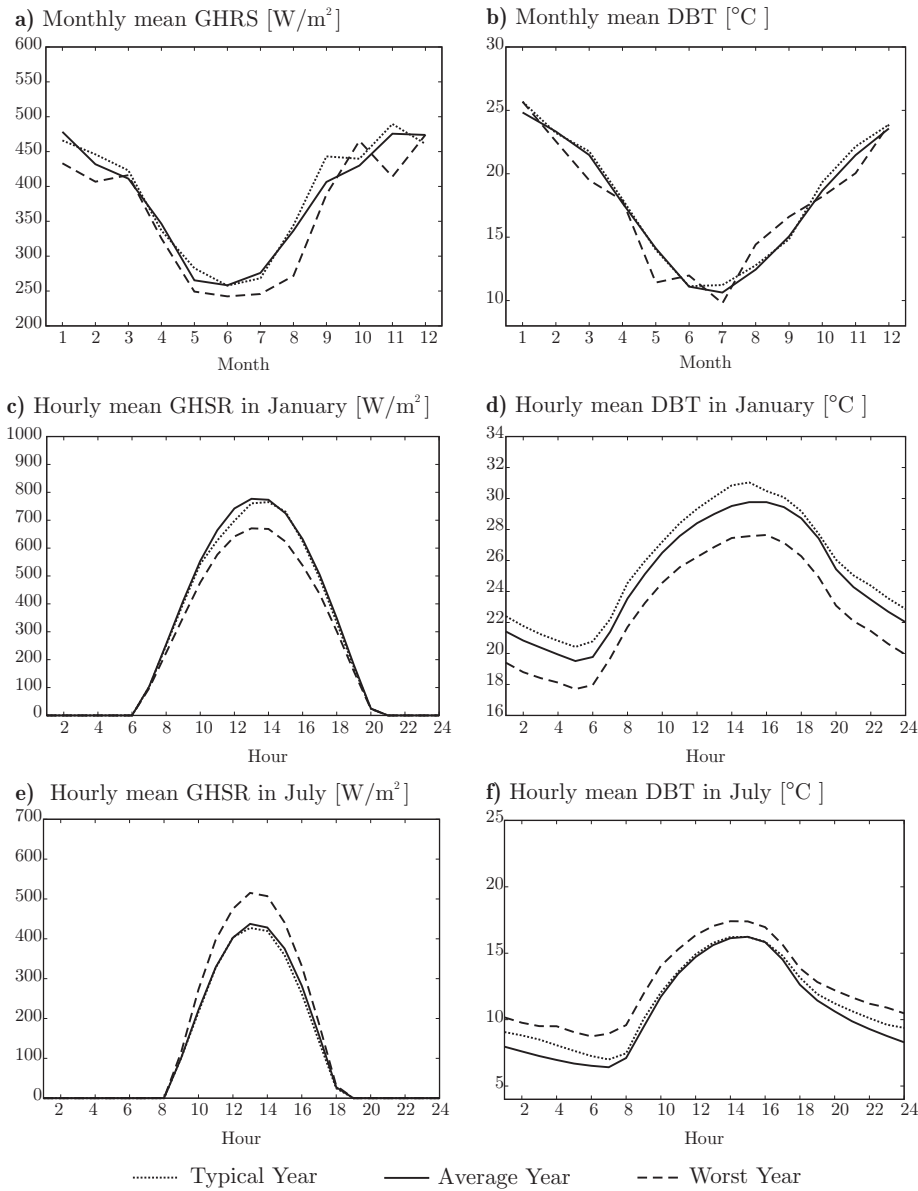
As a last approach to the long-term weather at Paraná, we directly take into account all the available (and usable) weather databases at Paraná for the period 1994–2014. Note that the current long-term database for Paraná has in average 18.5 usable years per month, as seen in Table 2. Therefore, BES using this database is about 18.5 more computationally expensive than BES using the TMY.

Fig. 8 shows the monthly cooling and heating loads computed using current TMY and the long-term database for Paraná, and the IWEC files for Buenos Aires and Asunción.

First, let us compare the results using the TMY with those ones using the long-term database for Paraná. Considering the cooling load, the results using the TMY are very close to the long-term results. The biggest difference is observed for August, one of the months with lowest cooling demand.

On the other hand, differences are relatively larger considering the heating loads. Qualitatively, the heating loads using the long-term database (with a peak for July at mid-winter) appear to be more accurate than those ones computed using the TMY (with a peak for May at autumn). Further, we did neither expect the heat load at Paraná to be higher than the one at Buenos Aires during May, nor the heating load at Paraná to be lower than the one at Asunción during September.

Then, let us compare the results at Paraná with those ones at Buenos Aires and Asunción.



**Fig. 7.** Comparison among the typical meteorological year, the average year, and the worst year in Rosario: (a, b) monthly mean global horizontal solar radiation and dry-bulb temperature, respectively; (c, d) hourly mean global horizontal solar radiation and dry-bulb temperature, respectively, in January (mid-summer); and (e, f) hourly mean global horizontal solar radiation and dry-bulb temperature, respectively, in July (mid-winter).

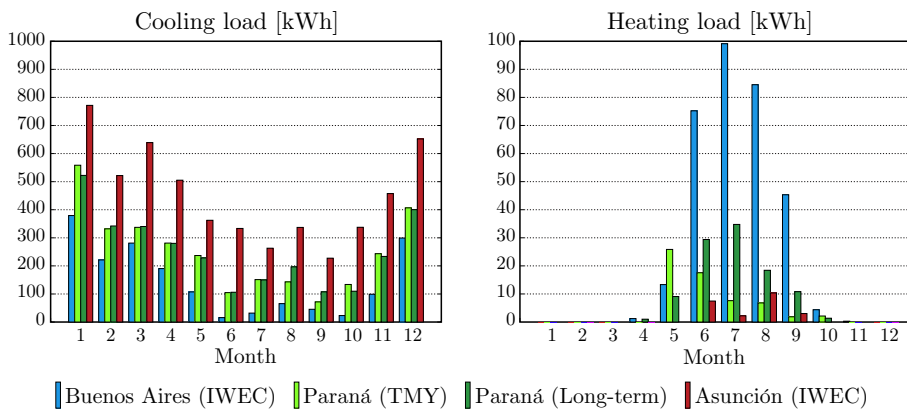


**Fig. 8.** Monthly cooling and heating loads for BESTEST-Case 910, as computed using the current defined TMY for Paraná, the long-term weather database for Paraná, and the IWECs files for Buenos Aires and Asunción.

Except for the unexpected heating loads computed using the TMY at Paraná for May and September, the cooling demand at Paraná is always higher than the one at Buenos Aires and lower than the one at Asunción, while the heating demand at Paraná is lower than the one at Buenos Aires and higher than the one at Asunción, which is logical considering that Paraná, Buenos Aires and Asunción have hot, warm temperate and very hot climate, respectively, as it can be seen in Fig. 1.

In any case, the differences between Paraná and the other locations, either in excess or in defect, are enormous all along the year, giving an additional proof of the usefulness of the current work.

Concerning the reported unexpected results for the heating load at Paraná during May and September, we will wait for having a longer database and making further tests to confirm whether they challenge the goodness of the respective TMMs or not. We just realise that, in case these TMMs are bad, this cannot be explained by the current choice of IWEC weighting factors since the TMMs chosen using the Sandia weighting factors were identical, as it can be inferred by observing Tables 8 and 9.

Meanwhile, keeping in mind that the heating loads are one order of magnitude lower than the cooling loads, we advocate for the validity of the current TMMs for September and May at Paraná until further evidence is available.

## 5. Conclusions

The first contribution of this work is the processing of the hourly weather databases provided by the Argentine National Meteorological Service (SMN) for 15 locations throughout the Argentine Littoral Region for the period 1994–2014. In general, these databases had gaps without measurements. Here, we rendered most of these incomplete databases usable for further analysis by using well-accepted data-filling methods, and discarded the others.

After processing, we built a large enough pool of complete hourly weather databases for each calendar month at 15 locations in Littoral.

But these databases still lack solar radiation data, which is available for only two locations in Littoral and for a few years. We circumvented the scarcity of solar radiation data by using the Zhang–Huang radiation model [9]. Further, we calibrate this model by fitting the available measurements to make it the most accurate for Littoral, the second major contribution of this paper.

In such a way, we obtained all the necessary weather data for the definition of the typical meteorological year (TMY) at 15 locations throughout Littoral, which is our final goal. We generated these TMYs, following the original Sandia method [13], as a concatenation of typical meteorological months (TMMs). Along the work, we tested different variants to the Sandia method, which finally led us to define the TMY in the same way as Thevenard and Brunge [6] defined the International Weather for Energy Calculations (IWEC).

As a contribution of this work to building energy simulation (BES), we converted these TMYs into the weather input format required by the energy simulation program EnergyPlus. And using EnergyPlus, we solved the BESTEST-Case 910 from ANSI/ASHRAE Standard 140-2011 at Paraná, located deep inside Littoral. For comparison purposes, the long-term weather at Paraná was characterised following two approaches: (1) using the current TMY, and (2) using the actual weather from the long-term database. Let us note that, from the computational point of view, the latter approach is considerably more expensive than the former one, and is usually unaffordable for real applications. Both approaches agreed on estimating the cooling load at Paraná all along the year. However, concerning heating loads, those computed using the TMY exhibited qualitatively unexpected values for two months. This, a priori,

challenges the validity of the corresponding TMMs (of course, at Paraná and in the light of the BESTEST-Case 910). But, considering that the heating load is considerably lower than the cooling load, we consider all the current TMMs for Paraná valid until further evidence.

Further, we solved this BESTEST for Asunción and Buenos Aires, which are the locations having typical weather (IWEC) files closest to Paraná. The resulting cooling and heating loads at these locations were sensibly different from those ones at Paraná, highlighting the importance of using a local TMY.

As future work, we will update the current TMYs as newer weather data will be available, and we will apply them for the energy simulation of a wide variety of cases, including further BESTESTs as well as real buildings, all around Littoral. By the way, we will address the questions arising from the just mentioned unexpected results on heating loads at Paraná.

## Acknowledgements

For the data supporting this work, we would like to thank the following institutions:

1. National Meteorological Service (SMN) of Argentina, for the weather measurements at 15 locations in the Argentine Littoral Region.
2. GerSolar (Research Group on Solar Radiation) at Universidad Nacional de Luján (UNLu), Argentina, for the solar radiation measurements at Paraná.
3. GER (Group on Renewable Energies) at Universidad Nacional del Nordeste (UNNE), Argentina, for the solar radiation measurements at Corrientes.

Further, the satellite-derived solar radiation data were obtained from the NASA Langley Research Center Atmospheric Science Data Center Surface meteorological and Solar Energy (SSE) web portal supported by the NASA LaRC project Prediction of Worldwide Energy Resource (POWER).

For funding this work, we would like to thank the following institutions:

1. Secretary for Science, Technology and Innovation (SECTEI) of the Province of Santa Fe, Argentina, via the project 2010-040-13 Res. SECTEI 117/13.
2. Universidad Nacional del Litoral (UNL), Argentina, via the project CAI+D 2011 50120110100441LI.

F. Bre is a doctoral student granted by the National Scientific and Technical Research Council of Argentina (CONICET).

## References

- [1] M.C. Peel, B.L. Finlayson, T.A. McMahon, Updated world map of the Köppen–Geiger climate classification, *Hydrol. Earth Syst. Sci.* 11 (2007) 1633–1644.
- [2] Instituto Argentino de Normalización y Certificación (IRAM), IRAM 11603, Acondicionamiento térmico de edificios. Clasificación bioambiental de la República Argentina (Thermal conditioning of buildings. Bioenvironmental classification of Republic Argentina), 2012.
- [3] Intergovernmental Panel on Climate Change (IPCC), *Climate Change 2014: Impacts, Adaptation, and Vulnerability. Part B: Regional Aspects. Contribution of Working Group II to the Fifth Assessment Report of the Intergovernmental Panel on Climate Change*, Cambridge University Press, 2014.
- [4] M.J. Scott, Y.J. Huang, Effects of climate change on energy use in the United States, in: *Effects of Climate Change on Energy Production and Use in the United States*, U.S. Climate Change Science Program and the Subcommittee on Global Change Research, Washington, DC, USA, 2007, Chapter 2.
- [5] R. Righini, A. Roldán, H. Grossi Gallegos, R. Aristegui, C. Raichijk, Nueva red de estaciones de medición de la radiación solar, in: XXXIII Reunión de Trabajo de la Asociación Argentina de Energías Renovables y Ambiente (ASADES), Cafayate, Salta, Argentina, 2010.



- [6] D.J. Thevenard, A.P. Brunger, The development of typical meteorological weather years for international locations: Part I, Algorithms, ASHRAE Trans.: Res. 108 (2002) 376–383.
- [7] Y.J. Huang, F. Su, D. Seo, M. Krarti, Development of 3012 IWEC2 weather files for international locations (RP-1477), ASHRAE Trans. 120 (Part 1) (2014) 340–355.
- [8] F. Kasten, G. Czeplak, Solar and terrestrial radiation dependent on the amount and type of cloud, Solar Energy 24 (2) (1980) 177–189.
- [9] Q. Zhang, J. Huang, S. Lang, Development of typical year weather data for Chinese locations, ASHRAE Trans. 108 (Pt. 2) (2002).
- [10] National Aeronautics and Space Administration (NASA), Surface meteorology and Solar Energy (SSE), 2014, URL <https://eosweb.larc.nasa.gov/cgi-bin/sse/grid.cgi>.
- [11] National Climatic Center (NCC), Test Reference Year (TRY), DSI-9706, 1976.
- [12] E.R. Hitchin, M.J. Holmes, B.C. Hutt, S. Irving, D. Nevrala, The CIBS example weather year, Build. Serv. Eng. Res. Technol. 4 (3) (1983) 119–124.
- [13] I.J. Hall, R.R. Prairie, H.E. Anderson, E.C. Boes, Generation of typical meteorological years for 26 SOLMET stations, Technical Report SAND 78-1601, Sandia National Laboratories, Albuquerque, New Mexico, USA, 1978.
- [14] W. Marion, K. Urban, User's Manual for TMY2s Typical Meteorological Years, National Renewable Energy Laboratory, U.S. Department of Energy, Golden, CO, USA, 1995.
- [15] S. Wilcox, W. Marion, Users Manual for TMY3 Data Sets, Technical Report NREL/TP-581-43156, National Renewable Energy Laboratory, U.S. Department of Energy, Golden, CO, USA, 2008.
- [16] G.J. Levermore, J.B. Parkinson, Analyses and algorithms for new test reference years and design summer years for the UK, Build. Serv. Eng. Res. Technol. 27 (4) (2006) 311–325.
- [17] D.J. Thevenard, A.P. Brunger, The development of typical meteorological weather years for international locations: Part II, Production/Discussion, ASHRAE Trans. 108 (2002) 480–486.
- [18] D.W. Crawley, Which weather data should you use for energy simulations of commercial buildings? ASHRAE Trans. 104 (2) (1998), TO-98-2-2, 1–18.
- [19] T. Lhendup, S. Lhundup, Comparison of methodologies for generating a typical meteorological year (TMY), Energy Sustain. Dev. XI (3) (2007) 5–10.
- [20] A.L.S. Chan, Generation of typical meteorological years using genetic algorithm for different energy systems, Renew. Energy 90 (2016) 1–13.
- [21] Various authors, EnergyPlus weather data, 2016. URL <https://energyplus.net/documentation>.
- [22] H. Alías, G. Jacobo, P. Martina, J. Corace, R. Borges, I. Yaccuzzi, F. Álvarez Palazzo, F. López, Monitoreo y simulaciones de desempeño térmico de aulas de la Facultad de Arquitectura de la UNNE en días de verano y condiciones reales de uso, Avances en Energías Renovables y Medio Ambiente 16 (5) (2012) 17–25.
- [23] M.L. Boutet, A.L. Hernández, G.J. Jacobo, Validación de simulaciones interactivas con SIMEDIF y ECOTECH, a partir de auditorías energéticas de un edificio escolar de la ciudad de Resistencia, Avances en Energías Renovables y Medio Ambiente 16 (2012) 27–34.
- [24] B. Garzón, C. Mendonca, Monitoreo y simulación térmica de dos viviendas sociales unifamiliares bajo condiciones reales de uso en la localidad de Colalao del Valle, Tucumán, Avances en Energías Renovables y Medio Ambiente 16 (2012) 05–39.
- [25] F. Bre, V.D. Fachinotti, G. Bearzot, Simulación computacional para la mejora de la eficiencia energética en la climatización de viviendas, Mecánica Computacional 32 (2013) 3107–3119.
- [26] M. Roriz, Arquivos Climáticos de Municípios Brasileiros, Associação Nacional de Tecnologia do Ambiente Construído (ANTAC), Grupo de Trabalho sobre Conforto e Eficiência Energética de Edificações, 2012, URL [http://www.roriz.eng.br/epw\\_9.html](http://www.roriz.eng.br/epw_9.html).
- [27] F. Bre, V.D. Fachinotti, Generación del año meteorológico típico para la ciudad de Santa Fe en la región Litoral Argentina, Avances en Energías Renovables y Medio Ambiente 18 (11) (2014) 01–08.
- [28] M. Krarti, J. Huang, D. Seo, J. Dark, Development of solar radiation models for tropical locations (ASHRAE Project RP-1309), American Society of Heating, Refrigerating and Air-Conditioning Engineers, Atlanta, GA, USA, 2006.
- [29] K.H. Kim, J.-C. Baltazar, J.S. Haberl, Evaluation of meteorological base models for estimating hourly global solar radiation in Texas, Energy Procedia 57 (2014) 1189–1198.
- [30] National Renewable Energy Laboratory (NREL), NSRDB Volume 1 – User's Manual – National Solar Radiation Data Base (1961–1990), Version 1.0, NREL, Golden, CO, USA, 1992.
- [31] American Society of Heating, Refrigerating and Air Conditioning Engineers (ASHRAE), ASHRAE® 2013 Handbook – Fundamentals, ASHRAE, Atlanta, GA, USA, 2013.
- [32] K. Skeiker, Generation of a typical meteorological year for Damascus zone using the Filkenstein–Schafer statistical method, Energy Convers. Manag. 45 (2004) 99–112.
- [33] Q. Zhang, Development of the typical meteorological database for Chinese locations, Energy Build. 38 (2006) 1320–1326.
- [34] T.F. Coleman, Y. Li, A reflective Newton method for minimizing a quadratic function subject to bounds on some of the variables, SIAM J. Optim. 6 (4) (1996) 1040–1058.
- [35] D.W. Marquardt, An algorithm for least-squares estimation of nonlinear parameters, J. Soc. Indust. Appl. Math. 11 (2) (1963) 431–441.
- [36] J.M. Finkelstein, R.E. Schafer, Improved goodness-of-fit tests, Biometrika 58 (3) (1971) 641–645.
- [37] F. Su, J. Huang, T. Xu, C. Zhang, An evaluation of the effects of various parameter weights on typical meteorological years used for building energy simulation, Build. Simulat. 2 (2009) 19–28.
- [38] A.L.S. Chan, T.T. Chow, S.K.F. Fong, J.Z. Lin, Generation of a typical meteorological year for Hong Kong, Energy Convers. Manag. 47 (1) (2006) 87–96.
- [39] D.B. Crawley, L.K. Lawrie, F.C. Winkelmann, W.F. Buhl, Y.J. Huang, C.O. Pedersen, R.K. Strand, R.J. Liesen, D.E. Fisher, M.J. Witte, J. Glazer, EnergyPlus: creating a new-generation building energy simulation program, Energy Build. 33 (4) (2001) 319–331.
- [40] Simulation Research Group at Lawrence Berkeley National Laboratory, Building Systems Laboratory at University of Illinois Urbana-Champaign, and other authors, Energyplus™ Documentation, v8.4.0 - Engineering Reference, 2015. URL <https://energyplus.net/documentation>.
- [41] R. Perez, P. Ineichen, R. Seals, J. Michalsky, R. Stewart, Modeling daylight availability and irradiance components from direct and global irradiance, Solar Energy 44 (5) (1990) 271–289.
- [42] Simulation Research Group at Lawrence Berkeley National Laboratory and Building Systems Laboratory at University of Illinois Urbana-Champaign, EnergyPlus™ Documentation, v8.4.0 - Auxiliary Energyplus Programs, 2015. URL <https://energyplus.net/documentation>.
- [43] R. Perez, P. Ineichen, K. Moore, E.L. Maxwell, R.D. Seals, A. Zelenka, Dynamic global-to-direct irradiance conversion models, ASHRAE Trans. 98 (Part 1) (2002) 354–369.
- [44] American Society of Heating, Refrigerating and Air Conditioning Engineers (ASHRAE), ANSI/ASHRAE Standard 140-2011: Standard Method of Test for the Evaluation of Building Energy Analysis Computer Programs, ASHRAE, Atlanta, GA, USA, 2011.